



Influence of Nano Particle Size on Attenuation and Dielectric Properties of Plantain Husk Powder Using Microwave Techniques at X-Band Frequency

Abubakar Yakubu^{1*}, Zulkifli Abbas², Olotu Olugbenga¹ and Suleiman Sahabi³

¹*Department of Physics, Kebbi State University of Science and Technology, Aliero, Nigeria.*

²*Department of Physics, Universiti Putra Malaysia, Serdang, Malaysia.*

³*Department of Science, State Polytechnic Dakingari, Kebbi State, Nigeria.*

Authors' contributions

This work was carried out in collaboration among all authors. Conceptualization, writing and statistical analysis of the work was done by Author AY. The methodology and manuscript editing was done by Author ZA. Morphological characterization was carried out by author SS while preparation of the samples were carried out by Author OO. All authors read and approved the final manuscript.

Article Information

DOI: 10.9734/PSIJ/2020/v24i530192

Editor(s):

(1) Dr. Bheemappa Suresha, The National Institute of Engineering, India.

(2) Dr. Thomas F. George, University of Missouri-St. Louis, USA.

Reviewers:

(1) Pankaj Shankar Kore, Shivaji University, India.

(2) Nagesh Sharma, Indian Institute of Technology, India.

Complete Peer review History: <http://www.sdiarticle4.com/review-history/58341>

Original Research Article

Received 19 April 2020

Accepted 23 June 2020

Published 07 July 2020

ABSTRACT

Ferrite are conventional materials used for microwave absorption, however, they are expensive, constitute health hazard and pollutes the environment. For these reasons, there is need to explore safe and environmental friendly materials that can serve as radiation absorbers and be used in fabricating microwave devices. In the light of the above, this work was geared towards exploring the use of Unripe Plantain Husk (UPH) waste material for microwave absorber applications. The usability was determined by investigating the dielectric properties and attenuation of the UPH powder with respect to particle size and frequency of operation. The nano particle of the UPH was prepared aseptically by washing in water and acetone, sliced, sundried and grinded. The grinded UPH powder was then subjected to high energy milling using a SPEX 8000D shaker for 4 hours, 8 hours, 10 hours and 12 hours. The milled powder was then prepared into pellets by suppressing with hydraulic press and mold which were then used for characterization. Results from investigation and analysis showed that the milled powder was in nano dimension using transmission electron microscope (TEM). The UPH powder sizes were in the range of 63.35 nm, 52.05 nm, 42.86 nm and

*Corresponding author: E-mail: abulect73@yahoo.com, abulec73@yahoo.com;

21.43 nm for the 4, 8, 10 and 12 hours milling, respectively. The dielectric constants for the as produced, 4, 8, 10 and 12 hours milled powder were 2.96, 4.97, 5.66, 6.97 and 10.36, respectively. The highest magnitude for attenuation was calculated for the 12 hours milled powder with a value of 14.92 dB and the least attenuation was calculated for the as produced powder with a value of 6.72 dB. Based on the results obtained it is concluded that nano particles of UPH powder is good for microwave attenuation and is a potential for fabricating electronic components.

Keywords: Attenuation; dielectric constant; unripe plantain husk; nano particles; microwave.

1. INTRODUCTION

The application of Electromagnetic (EM) waves are found in many applications in numerous areas such as wireless communication systems, radar, local area network, electronic devices, mobile phones, laptops and medical equipment's at microwave frequencies [1]. Due to technological advancement in telecommunication and other electronic devices, electromagnetic interference (EMI) is now a challenge which must be suppressed to acceptable absorption limits. EMI reducing materials (absorbers) may be dielectric or magnetic and the design depends on the frequency range, the desired quantity of shielding and the physical characteristics of the devices being shielded. EMI could be suppressed by using waste materials that possess good or enhanced electrical and mechanical properties [2].

Microwave absorbers are materials that attenuate the energy in electromagnetic waves (EM) and are used to suppress EMI. Ferrite based microwave absorbers absorb the EM energies that propagates through it, converts and dissipates those energies as heat, however, ferrites have been reported to be toxic to humans and environment [3]. Microwave absorbing materials can be manufactured by a number of dielectric materials in powder/solid form, loaded with various kind of polymeric binder [4]. For microwave applications, many studies have been focused on the suitability of agricultural waste materials and whether they are fully biodegradable, environmentally friendly, abundantly available, renewable, and cheap and of low density.

It is reported that the proximate chemical composition of UPH are lignin, amino acid, cellulose (10%) and hemicellulose (13%), protein (15%) and iron (20%) [5]. The iron content in the UPH influences the electromagnetic properties of the nano husk powder. Based on findings and reports of several investigations on microwave absorber, it is necessary to explore new material

suitable for microwave absorption. This new material should meet standards of being biodegradable, environmentally friendly, abundantly available, renewable, and cheap [6]. In the light of the above UPH was selected as a materials possible to attenuate EM at microwave frequency.

Conventional technique to measure microwave properties is filling a section of a standard closed transmission line such as a waveguide. However, in this technique it is extremely difficult to fit tightly solid materials into a waveguide without leaving air gaps especially for fragile materials like fibers. The microstrip transmission method is a good measurement technique in a wide band frequency range due to its simplicity in set-up and sample placement in the strip [7]. The microstrip transmission method is one of planar transmission line method since the materials can be easily loaded in the measurement test fixture. The microstrip transmission line is based on a reflection and transmission technique adapted to a two port microstrip transmission line [8].

2. THEORY

For two-port network in scattering parameter measurement, the wave variables are defined as [4];

$$S_{11} = \left. \frac{b_1}{a_1} \right|_{a_2=0} \quad S_{12} = \left. \frac{b_1}{a_2} \right|_{a_1=0} \quad (1)$$

$$S_{21} = \left. \frac{b_2}{a_1} \right|_{a_2=0} \quad S_{22} = \left. \frac{b_2}{a_2} \right|_{a_1=0} \quad (2)$$

Where, $a_n = 0$ indicates that there is a perfect impedance match meaning there is no reflection from terminal impedance at port n . The expression in equation (1) and (2) may be rewritten as;

$$\begin{bmatrix} b_1 \\ b_2 \end{bmatrix} = \begin{bmatrix} S_{11} & S_{12} \\ S_{21} & S_{22} \end{bmatrix} \begin{bmatrix} a_1 \\ a_2 \end{bmatrix} \quad (3)$$

Where, the matrix containing the S parameters is referred to as the scattering matrix, which is simply denoted by [S].

The parameters directly measurable at microwave frequency are S_{11} and S_{22} called the reflection and S_{12} and S_{21} called the transmission coefficients. Scattering parameters are complex in terms of magnitude. However, they mostly expressed in terms of amplitudes and phases. Often their amplitudes are given in decibels (dB), which are defined as;

$$S_{mn} = |S_{mn}|e^{j\theta_{mn}} \quad (4)$$

Where $m = 1$, and $n = 2$.

Equation (4) when written in the form of decibel will give;

$$dB = -20 \log(S_{mn}) \quad (5)$$

Thus, the attenuation of materials can be calculated using the formula given in equation (5).

$$Attenuation (dB) = -20 \log(S_{21}) \quad (6)$$

The measurement with the microstrip transmission line entails placing the sample flat on the strip line without any air gap then the flanges of the microstrip are connected to the (vector network analyser (VNA) via port 1 and port 2. The result obtained for the transmission coefficients (S_{21}) is then used to compute the attenuation of the material under study using equation (6). Transmission coefficient (S_{21}) measurement setup is shown in Fig. 1 (a & b). The setup consists of a microstrip antenna and an Agilent N5230A PNA-L.

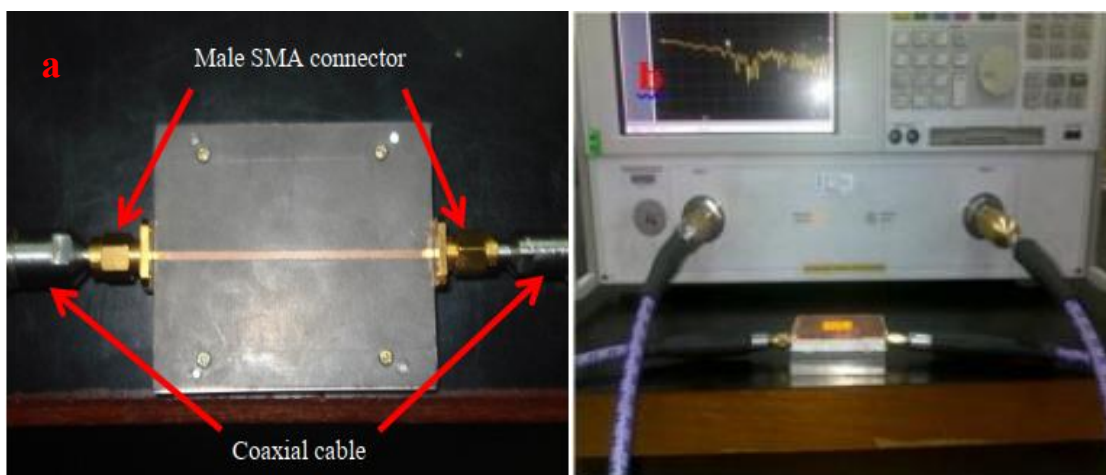


Fig. 1. (a) Microstrip antenna (b) S_{21} measurement setup

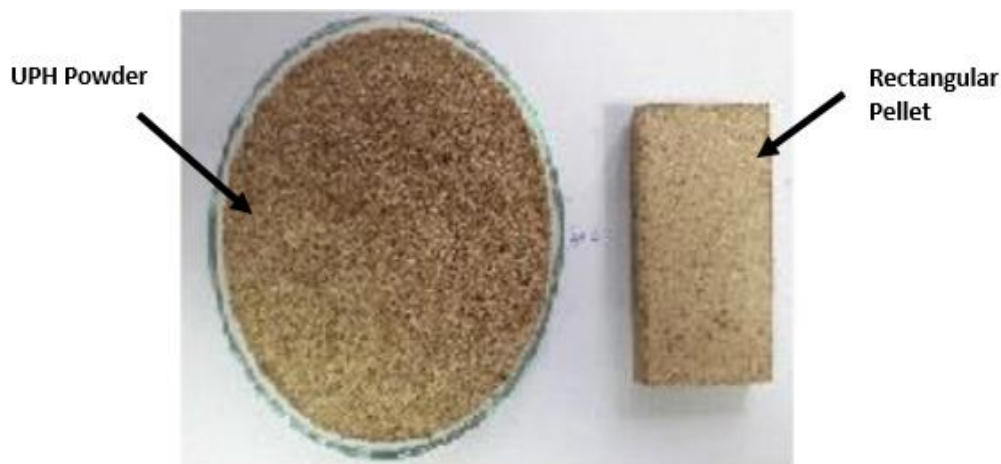


Fig. 2. Milled and compressed UPH powder

3. METHODOLOGY (SAMPLE PREPARATION)

UPH nano powder was prepared by mechanical alloying technique after washing the husk in water and acetone, sundried and grinded. The grinded UPH powder was then sieved to a dimension of 200 μm . 40 g of the 200 μm was then mechanically alloyed using high energy milling in SPEX 8000D shaker for 4, 8, 10 and 12 hours each. The 8000D shaker was operated at 1400 rpm by a 50 Hz motor at a clamp speed of 875 cycles/minute using a ball to powder ratio of 10:1. The milled powder was then prepared into rectangular pellets of 8 mm thickness for each milling time using hydraulic press and block mold specifically constructed for this purpose. The thickness chosen is as recommended by Agilent Technologies for pellets measurement involving microstrip transmission lines. The samples milled at different milling times were analyzed using Transmission electron microscope (TEM), and Atomic Force Microscope (AFM) to study their surface morphology. Fig. 2 is the grinded UPH powder before mechanical alloy and pellet of the milled UPH nano powder.

Measurements of the dielectric constant and loss factor of the milled powder was done at room temperature using Agilent 85070B open ended coaxial probe (OEC) which was connected to a high accuracy coaxial cable to an Agilent N5230A PNA-L vector network analyzer (Agilent Technologies, CA, USA) at X-band frequency. For calibration, a 3.5 inch high density shorting block and distilled water at 25°C were

used for a one-port reflection-only system. The calibration was verified by measuring the permittivity of water (standard material) and comparing the results with manufacturer's values. Good agreement of the measurement results for water and that of manufacturer's value means perfect calibration. Shown in Fig. 3 is the measurement set-up for complex permittivity measurement. The open ended coaxial probe is firmly placed on the surface of the pellet to determine their complex permittivity using the equipment's software.

4. RESULTS AND DISCUSSION

4.1 Surface Morphology

4.1.1 Transmission electron microscope

TEM micrograph shown in Fig. 4 is of the UPH nano powder obtained from the milling process for the different milling hours. The as produced samples before milling was measured to be 200 μm using a sieve. Observation on the milled samples showed that as milling hour increases, a smaller particle size begins to emanate due to the thermal energy supplied in the vial during the milling. Analysis showed that grain disintegrated from micro meter sizes to nano dimension after 4 hours of mechanical milling. The particle size distribution obtained from TEM micrographs showed that the average particles sizes are 63.35 nm, 52.05 nm, 42.86 nm and 21.43 nm for the 4, 8, 10, and 12 hours milling hour, respectively.

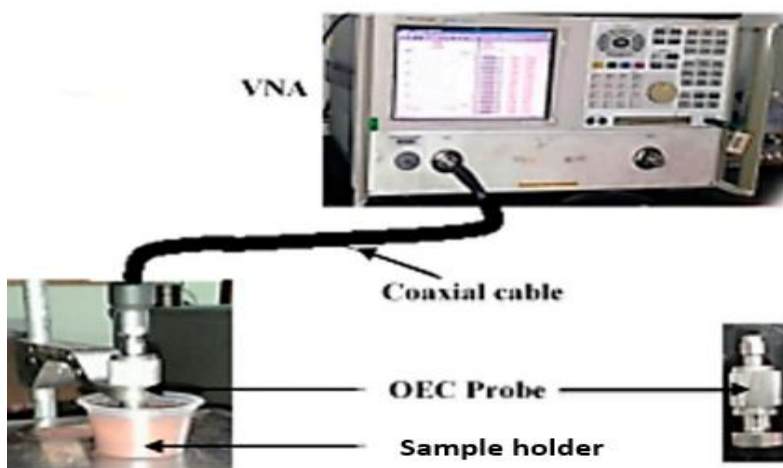


Fig. 3. Measurement setup for dielectric constant and loss factor

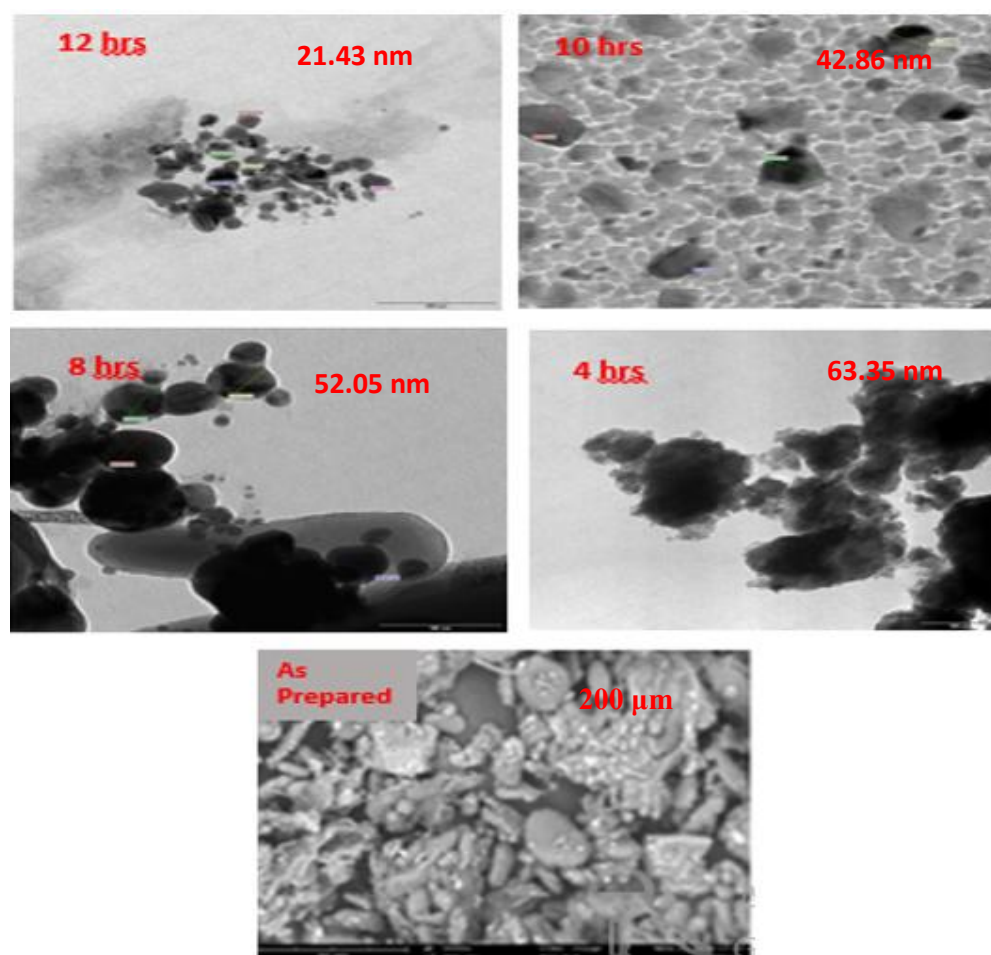


Fig. 4. TEM micrographs for all samples prepared

4.2 Atomic Force Microscope

Atomic force microscopic analysis is used in this work to study the nano-metric dimensional surface roughness and for visualizing the surface texture. The surface of the UPH nano powder were measured at a horizontal scale of $2\ \mu\text{m}$ and vertical scale of $50\ \text{nm}$. Shown in Fig. 5 is a two-dimensional (2D) AFM images for the UPH samples for milling hours of 4 to 12 hours which depicts grooves and valleys. Further observation showed that powder surface morphology at 12 hours is smoother than that of the other milling hours which is attributed to grain disintegration. [9] described that longer milling hours can stimulate the migration of grain boundaries and cause the coalescence of more grains during the milling processes which in-turn causes domain walls development. The surface roughness of the nano UPH pellets decreased from 26.52 to $15.07\ \text{nm}$ as the milling hours increased from 4 to 12

hours. Based on AFM analysis, the surface roughness of the samples is considered smooth since the roughness was in nm scale proposing that the samples are good for electromagnetic propagation with regards to sample surfaces.

4.3 Complex Permittivity

Shown in Fig. 6 is the dielectric constant for the as prepared sample and the nano powder of different milling hours. Careful observation showed that the dielectric constant decreased sequentially as frequency increased from 1 to 20 GHz. The declivity was attributed to material polarization due to continuous divergent electric field [4]. Due to the accumulation of charges created by the dense surface of the nano UPH, there tends to be higher dielectric constant which was excited by the interaction between the materials and electromagnetic waves [4].

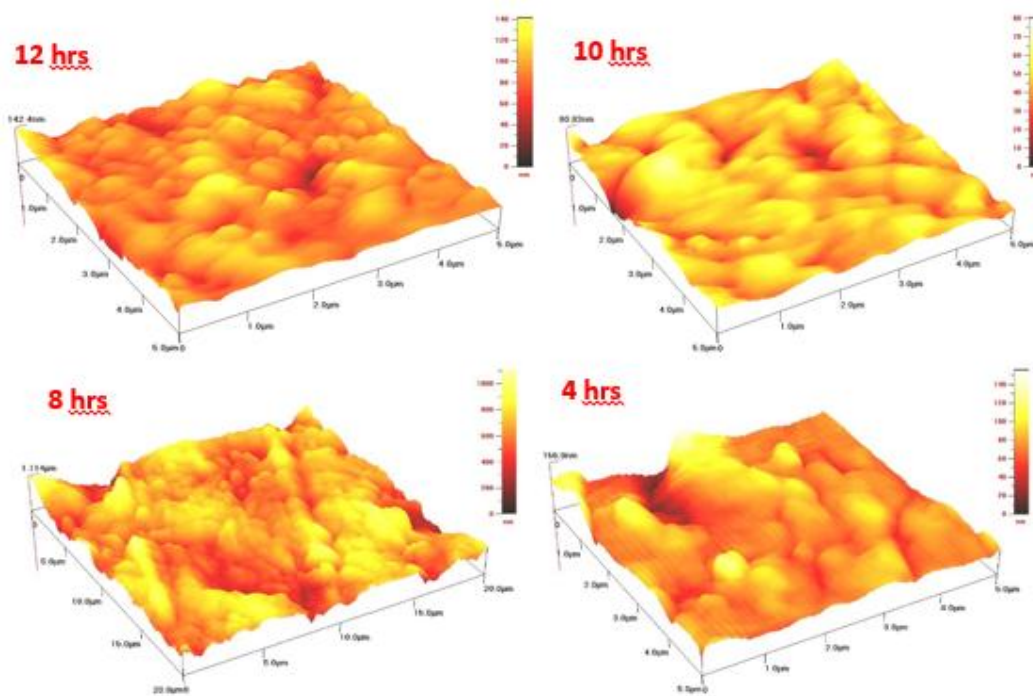


Fig. 5. AFM micrographs for the nano samples prepared

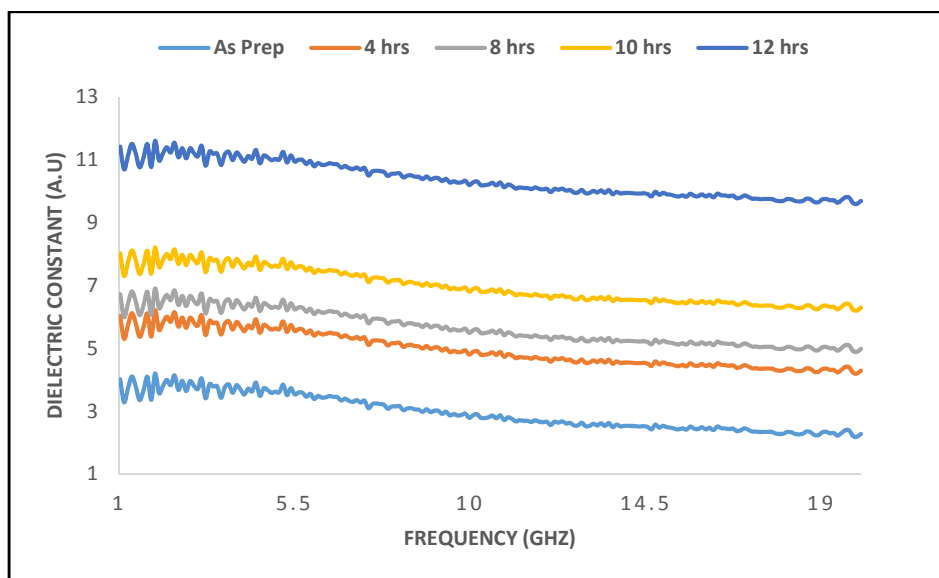


Fig. 6. Dielectric constant of samples prepared

Further analysis showed that materials with the least powder size had the highest dielectric constant. The reduction of dielectric constant at high frequencies must have been influenced by the gradual decrease in the orientation change or dipole movement at high frequencies [10]. The

amount of lignin and iron constituents in the UPH also influenced the dielectric constant. The average dielectric constant for the samples were observed to be 2.96, 4.97, 5.66, 6.97 and 10.36 for the as prepared, 4, 8, 10 and 12 hours milled samples, respectively. The behavioral trend of

the samples with respect to milling hours can be clearly seen in Fig. 7. This results confirms that nano materials of microwave absorbing UPH are better than those of other fibers where oil palm fibers (OPEFB) highest dielectric constant was reported to be 3.65 [11].

Careful observation on Fig. 8, shows the gradual increase in loss factor as milling hour increases. The general decrease in loss factor as frequency

increases is attributed to material polarization orientation also associated to the UPH chemical constituents [12]. From analysis, it is then concluded that loss factor depends on the dimension of material and frequency of operation. The switchback-shaped line for the loss factor is visible in all sample sizes which is evidence of mismatch theory between the measuring flange of the VNA and sample surfaces [13].

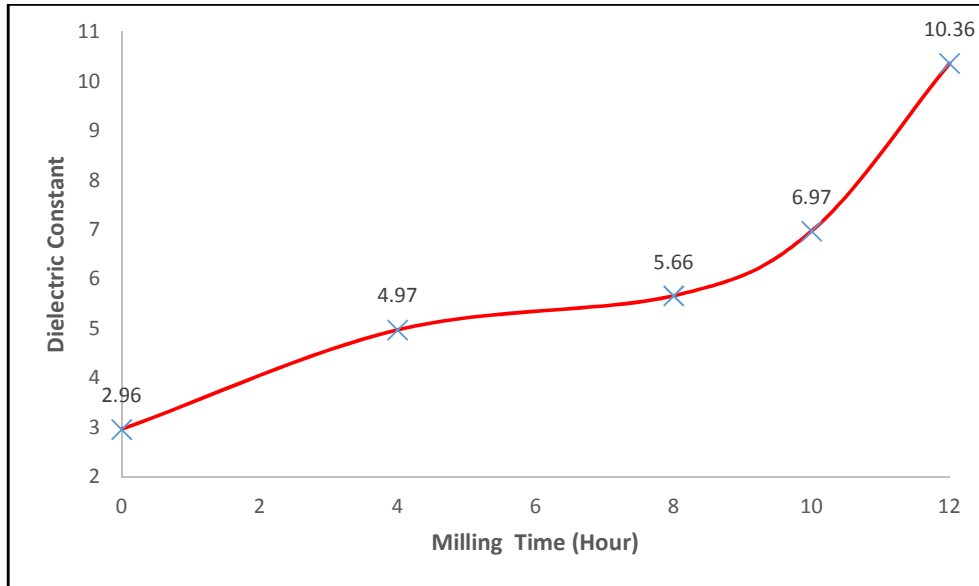


Fig. 7. Milling time vs average dielectric constant

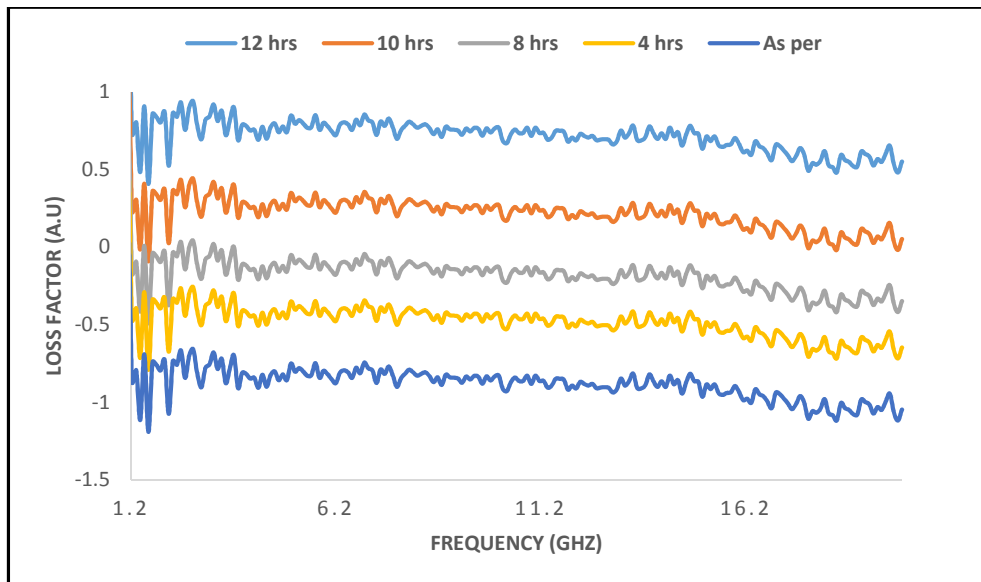


Fig. 8. Loss factor of prepared samples

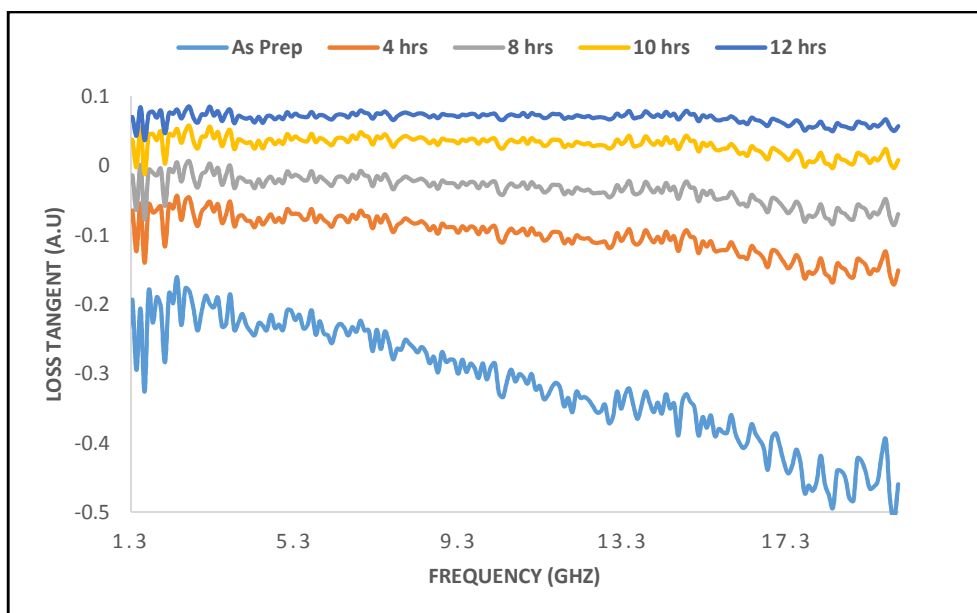


Fig. 9. Loss tangent of prepared samples

The graph shown in Fig. 9 represents the loss tangent and it depicts a ripple like trend at lower milling hours which might be due to voids in the suppressed sample. The change in loss tangent as milling hour's increases may be attributed to different physical properties, such as the particle size, material density and surface dispersion [14]. The loss tangent for all the samples indicated that, the ordered behavior of the

particle sizes was due to the increasing frequencies and sample particle rearrangement [6]. The highest loss tangent was obtained at the lowest frequency, for the 12 hours milled sample with a value of 0.6. The steep dive by the 200 μm powder (as prepared) simply shows that nano materials are better than micrometer in electromagnetic suppression.

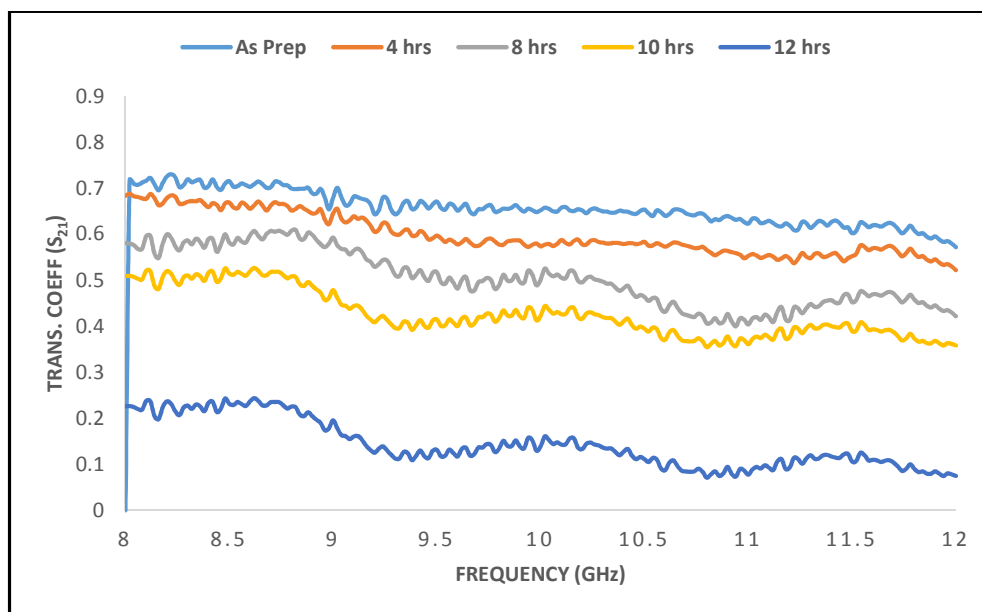


Fig. 10. Transmission coefficient of samples prepared

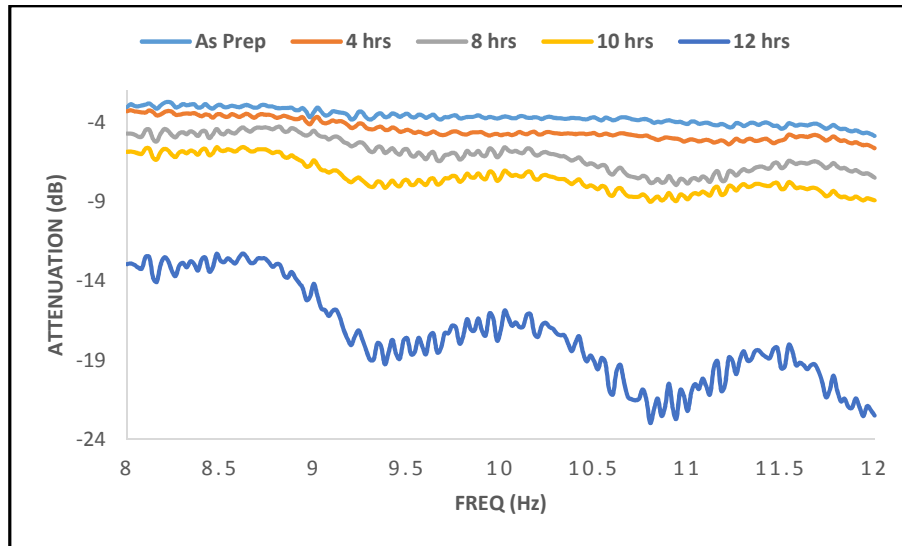


Fig. 11. Attenuation of samples

4.4 Transmission Coefficient (S_{21})

The increase in S_{21} magnitude as milling hours increases is clearly distinguishable from one sample to another. Observation shows that there is high absorption of electromagnetic waves which propagates through sample at the higher milling hours, thereby leading to diminished transmitted waves. This behavior is in agreement with the impedance mismatch theory which states that the higher the dielectric properties of a material, the lower its magnitude of transmission coefficient [15]. The result in Fig. 10 clearly support the results in Fig. 6, where the powder with the highest dielectric constant then tend to absorb more energy of the electromagnetic waves that were propagating through the samples.

4.5 Attenuation of Samples

The X-band spectra for attenuation were calculated using the the formula in equation (6). The calculated attenuation of the UPH nanopowder is shown in Fig. 11. Observation on Fig. 11 showed that attenuation at 8 GHz for the UPH powder ranges from -3.1 to -12.9 dB and the values at 12 GHz ranges from -4.9 to -22.5 dB. There was a clear indication of a sharp increase in attenuation as milling hour increased. The increase is attributed to the disintegration of the powder samples resulting in increased surface area hence increasing the attenuation of the nano UPH powder [16]. In electronic devices, standard attenuation values can be ranged from

-0 to -60 dB with frequency maximums that range from 1 to 50 GHz depending on attenuators type [13]. Based on the standard reported, the UPH material produced is good for attenuation, especially at low and medium shielding applications.

5. CONCLUSION

High quality nano powder was synthesized from waste material of UPH using high energy ball mill at different hours thereby enhancing its size from micrometer to nano meter scale. The milling procedure produced sequential increase in dielectric constant and attenuation as milling hour's increases. The gradual increase in attenuation and dielectric constant made the UPH nano powder a potential player in electromagnetic microwave absorbing materials. The microstructural evolution of the milled powder as particles disintegrated, facilitated the improvements in the electromagnetic properties of UPH nano samples.

The surface morphology displayed by the nanopowder confirmed their ability to attenuate microwaves in the X-band frequency range. The significant electromagnetic properties of the UPH nano powder can be employed in possible applications requiring tunable attenuation of electromagnetic energy. This material with improved dielectric and attenuation properties are cheaper to produce, lighter, biodegradable, abundantly available and environmentally friendly and could reduce the limitations associated with

the ferrites commonly used in microwave absorption applications. The UPH nano material can be prepared into sheets and fabricated as printed circuit boards and covers for EMI radiating devices.

ACKNOWLEDGEMENTS

The authors wish to thank the Department of Physics, Kebbi State University of Science and Technology, Aliero, Nigeria and the Department of Physics, Universiti Putra Malaysia for providing facilities for the research.

COMPETING INTERESTS

Authors have declared that no competing interests exist.

REFERENCES

- Mobashsher AT, Abbosh AM. Artificial human phantoms: Human proxy in testing microwave apparatuses that have electromagnetic interaction with the human body. *IEEE Microwave Magazine*. 2015;16(6):42-62.
- Ahmad AF, Aziz SA, Obaiys SJ, Zaid MH, Matori KA, Samikannu K, Aliyu US. Biodegradable Poly (lactic acid)/Poly (ethylene glycol) reinforced multi-walled carbon nanotube nanocomposite fabrication, characterization, properties and applications. *Polymers*. 2020;12(2): 427.
- Esa F, Abbas Z, Fadhil OA, Yakubu A, Jusoh MA. Influence of nickel-zinc ratio on power loss of $\text{Ni}_x\text{Zn}_{1-x}\text{Fe}_2\text{O}_4$ using microstrip technique at microwave frequency. *International Journal of Microwave and Optical Technology*. 2015;10(2).
- Yakubu A, Abbas Z, Esa F, Tohidi P. The effect of ZnO nanoparticle filler on the attenuation of ZnO/PCL nanocomposites using microstrip line at microwave frequency. *International Polymer Processing*. 2015;30(2):227-232.
- Shadrach I, Banji A, Adebayo O. Nutraceutical potential of ripe and unripe plantain peels: A comparative study. *Chemistry International*. 2020;6(2):83-90.
- Abdalhadi DM, Abbas Z, Ahmad AF, Ibrahim NA. Determining the complex permittivity of oil palm empty fruit bunch fibre material by open-ended coaxial probe technique for microwave applications. *BioResources*. 2017;12(2): 3976-91.
- Abdulkarim YI, Deng L, Karaaslan M, Altıntaş O, Awl HN, Muhammadsharif FF, Liao C, Unal E, Luo H. Novel metamaterials-based hypersensitized liquid sensor integrating omega-shaped resonator with microstrip transmission line. *Sensors*. 2020;20(3):943.
- Kang TG, Park JK, Kim BH, Lee JJ, Choi HH, Lee HJ, Yook JG. Microwave characterization of conducting polymer PEDOT: PSS film using a microstrip line for humidity sensor application. *Measurement*. 2019;137:272-7.
- Enayatzadeh M, Mohammadi T, Fallah N. Influence of TiO_2 nanoparticles loading on permeability and antifouling properties of nanocomposite polymeric membranes: Experimental and statistical analysis. *Journal of Polymer Research*. 2019;26(10): 240.
- Pan C, Kou K, Jia Q, Zhang Y, Wu G, Ji T. Improved thermal conductivity and dielectric properties of hBN/PTFE composites via surface treatment by silane coupling agent. *Composites Part B: Engineering*. 2017;111:83-90.
- Shamsuri AA, Awing MI. An initial investigation on microwaves reflection and transmission coefficients of oil palm empty fruit bunch biocomposites incorporated with nickel zinc ferrite. *Journal of Materials Science Research and Reviews*. 2020;42-9.
- Klygach DS, Vakhitov MG, Suvorov PV, Zherebtsov DA, Trukhanov SV, Kozlovskiy AL, Zdorovets MV, Trukhanov AV. Magnetic and microwave properties of carbonyl iron in the high frequency range. *Journal of Magnetism and Magnetic Materials*. 2019;490:165493.
- Pozar DM. *Microwave Engineering*. John Wiley & Sons; 2012.
- Fernández Perdomo CP, Zabotto FL, García D, Kiminami RH. Effect of the CoFe_2O_4 initial particle size when sintered by microwave on the microstructural, dielectric and magnetic properties. *International Journal of Applied Ceramic Technology*. 2019;16(5):2073-84.

15. Wang Z, Chen H, Nian W, Fan J, Li Y, Wang X, Ma X. Grain boundary effect on dielectric properties of (Nd_{0.5}Nb_{0.5})_xTi_{1-x}O₂ ceramics. *Journal of Alloys and Compounds*. 2019;785:875-82.
16. Tekin HO, Sayyed MI, Altunsoy EE, Manici T. Shielding properties and effects of WO₃ and PbO on mass attenuation coefficients by using MCNPX code. *Dig J Nanomater Biostruct*. 2017;12(3):861-7.

© 2020 Yakubu et al.; This is an Open Access article distributed under the terms of the Creative Commons Attribution License (<http://creativecommons.org/licenses/by/4.0>), which permits unrestricted use, distribution, and reproduction in any medium, provided the original work is properly cited.

Peer-review history:

The peer review history for this paper can be accessed here:
<http://www.sdiarticle4.com/review-history/58341>